25th ABCM International Congress of Mechanical Engineering
October 20-25, 2019, Uberlândia, MG, Brazil

COB-2019-1489
TRIBOLOGICAL EVALUATION OF NI-CR-B-SI COATINGS DEPOSITED BY LASER METAL DEPOSITION AND TREATED BY LASER REMELTING

Jurandir Marcos Sá de Sousa
Adriano de Souza Pinto Pereira
Rafael Gomes Nunes Silva
Calil Amaral
Milton Pereira
Universidade Federal de Santa Catarina, Mechanical Engineering Department, Precision Engineering Laboratory - Laser
marcos.jurandir@yahoo.com.br
adriano.sppereira@gmail.com
rafaelnunes.mat@hotmail.com
amaral.calil@gmail.com
eng.milton@gmail.com

Abstract. *Industrial development is constantly opposed by problems related to the action of wear mechanisms. Among these, it is possible to emphasize adhesive wear, responsible for generating financial losses in several sectors. One way to reduce this loss has been the application of wear resistant coatings, usualy composed by alloys with dedicated properties and deposited by processes capable of delivering the desired characteristics. Ni-based alloys coatings deposited via laser metal depostion (LMD) have been know to performed well in this scenario, increasing components lifespan and consequently reducing production and repair costs. Although most of these coatings already present good results in its microstructure, hardness and tribological behavior, some can be improved by post-deposition treatments, such as laser remelting. In this ambit, the present research compares and analyses the tribological behavior of a Ni-Cr-B-Si coating deposited by LMD and its laser remelted equivalent. The coatings' occurence of superficial macro defects, their microhardness and tribological performance in the ASTM G99 test were compared. Friction coefficients (load cell), volumetric loss (optical interferometry), Archard's coefficients and worn surfaces, analysed via SEM and EDX, were evaluated. Results show that the laser remelting treatment was effective in reducing cooling cracks, increasing hardness and reducing friction coefficient and volumetric loss.*

Keywords: *Adhesive Wear, Wear Resistant Coatings, Ni-based Alloys, Laser Remelting, Cooling Cracks.*

1. INTRODUCTION

Intense industrial growth requires constant material development to enhance the most diverse applications. Work components or implements subjected to adhesive wear are common and are no exception to the previous statement. Generally, to reduce wear, these applications need exposed surfaces with high hardness values and good roughness quality, which, by their turn, avoid the occurrence of high friction coefficients (COF), wear rates and the joint interaction between wear mechanisms (Zum Gahr, 1987) and (Hutchings; Shipway, 2017). This interaction accelerates the components deterioration process, reducing their lifespan and consequently increasing repair and replacement costs.

Coatings application with desired and specific properties have proven to be a good alternative, both operationally and financially. Such allows preparation of only the surface that will be directly exposed to wear condition, dispensing the integral component manufacture from a noble alloy, resource that drastically reduces production costs. Wear resistant coatings can be deposited by thermal spray and arc welding techniques. However, such coatings may generate, in a number of conditions, lack of metallurgical adhesion, extensive heat-affected zone (HAZ) and high dilution. These aspects are emphasized from well-established literature until more recent works (Toyserkani et al., 2005), (Zhong; Liu, 2010), (Davim, 2013), (Houdková et al., 2014), (Da Silva; D'Oliveira, 2016), (Sousa et al., 2018) and (Zhao et al., 2018).

Literature indicates that the laser metal deposition (LMD) technique can generate coatings which are successful in facing these processing problems. LMD's advantages derive from the unique laser radiation properties, which generates a highly directional beam, high maximal available power, versatility and high achievable energy density. Ni-Cr-B-Si alloys, in their turn, are capable of simultaneously providing resistance to abrasive, adhesive and corrosive wear mechanisms.

Laser remelting process is a technique belonging to the laser post processing method (that includes, among others, remelting, texturization, heat treatments). In such a laser beam is irradiated in the target surface in order to remelt a thin material layer, generating a molten pool (Houdková et al., 2014 and Marimuthu et al., 2015). The surface tension from this molten pool causes portions of the material`s roughness peaks to flow into valleys, making the surface more uniform, homogeneous and flat. Besides improving metallurgical aspects, which standardizes the surface thermal cycle, generating better mechanical properties distribution along the coating (Temmler et al., 2015). In this process, there is no removal, only material reallocation (Yin et al., 2011 and Zhao et al., 2018).

In order to analyze the combination of Ni-Cr-B-Si alloy class properties, involving LMD deposition and a laser remelting post-treatment, this work evaluated the tribological wear resistance of a Ni-Cr-B-Si alloy coating deposited via LMD in two different conditions, with and without laser remelting post-treatment. Despite the advantages highlighted, the alloys included in this class are highly susceptible to cooling cracks appearance (Houdková et al., 2014 and Sousa et al., 2018). The deposition process and post laser surface treatments have high parameterization complexity due to the large number of variables involved (Davim, 2013). Thus, through the processing of a commercially available alloy and a single bead design of experiment, a suitable LMD parameter was identified and used to deposit the final coating, as well as for the remelting treatment application. Subsequently, surface aspects assessments, hardness and tribological behavior inference were carried out. This article aims to contribute to this discussion.

2. MATERIALS AND METHODS

Experimental procedures are divided into four steps: (1) single beads preliminary tests to define the coatings deposition parameters; (2) coating deposition process; (3) application of remelting post-treatment in half the samples available; (4) microhardness test and dry medium pin-on-disk tribological testing on all samples, following the ASTM-G99 (2017) standard requirements.

2.1 Single beads preliminary tests to define LMD processing parameters

ASTM A36 material - carbon steel drawn discs were used as substrate dimensions (Ø 50,0 mm x δ 10,0 mm). After their surfaces were prepared by abrasive blasting, ethyl alcohol cleaning and drying, substrate samples received the preliminary single beads tests. An experimental matrix, with six laser power levels, *P* (0.35-2.10 kW, with steps of 350 W) and four processing speed levels, *V* (5.0-30.0 mm/s), with steps of 8.3 mm/s was chosen to compose the preliminary single beads tests, while other parameters were kept constant. Coating material consists of the NiCrBSi 1545-00 alloy produced by Höganäs S.A. The powder particle size range is -106 +53 μm and chemical composition wt %: 0.3-0.4 (C); 2.0-3.4 (Fe); 7.5-10 (Cr); 1.7-2.0 (B); 3.3-3.9 (Si) and (N) in balance.

The single beads resulting from the preliminary tests were cross-sectioned, subjected to a conventional metallographic process (grinding, polishing with alumina and chemical etching in 2% nital reagent). Micrographies were taken from these sections in a LEICA EC3 optical microscope. Using the ImageJ® software, single bead dilution and other geometric aspects were measured: height (*h*), width (*W*), area (*A*), penetration (*p*) and wetting angle (β). It was also evaluated the presence of defects and discontinuities, such as cracks, pores and detachments (lack of fusion).

2.2 Coatings deposition process

Both the fore-described single beads and the final coatings were deposited using a YLS-10000 IPG PHOTONICS® fiber laser source and the following fixed parameters: powder feed rate, 10.4 g/min; laser beam diameter at focus, 0.8 mm; shielding gas flow (Ar), 15 l/min and carrier gas flow (Ar), 5 l/min. The overlap rate for the final coatings, set as 30%, was chosen through simulations performed in MATLAB® software, in a program developed within the LMP-Laser group. The algorithm was developed based on the work presented by Ocelík et al. (2014). After inserting the data (clad height - mm, clad width - mm, overlap rate to be tested - %, number of clad tracks and layers and Ni-Cr-B-Si alloy density and surface tension), the cross section with the best geometric aspect was chosen to deposit the final coating, as shown in Figure 1.

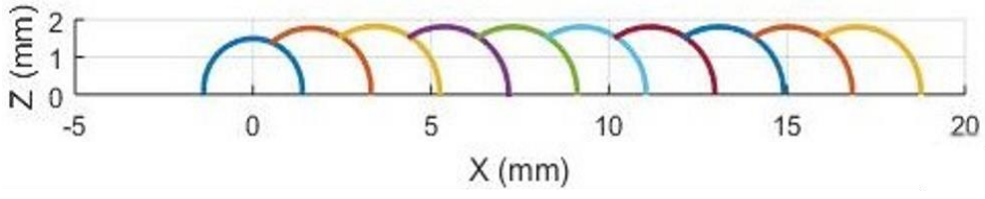

Figure 1. Cross section chosen for the coating deposition based on overlap predictions via MATLAB® software.

Among the 24 single beads evaluated, parameters set with the best performance was chosen based in the measured properties described in topic 2.1: low dilution, proper *h* and *w* values, a considerable *A* (important for productivity), low *p*, β lower as to 90° (to avoid lack of fusion in overlapping) and cracks, pores and detachments absence. Thus, the final coatings were deposited using *P* and *V* equal to 1.05 kW and 5.0 mm/s, respectively.

2.3 Application of remelting post-treatment in half the sample space

Four samples were coated with the chosen parameters, however, two were also subjected to the remelting treatment. To accomplish this, the following was executed: immediately after the coating layer deposition, the powder feed was ceased and, using only laser beam and keeping the parameters constant, the coating surface was traversed and swept by laser beam, generating the remelting in the same concentric pattern as the deposition. Figure 2 illustrates these two steps.

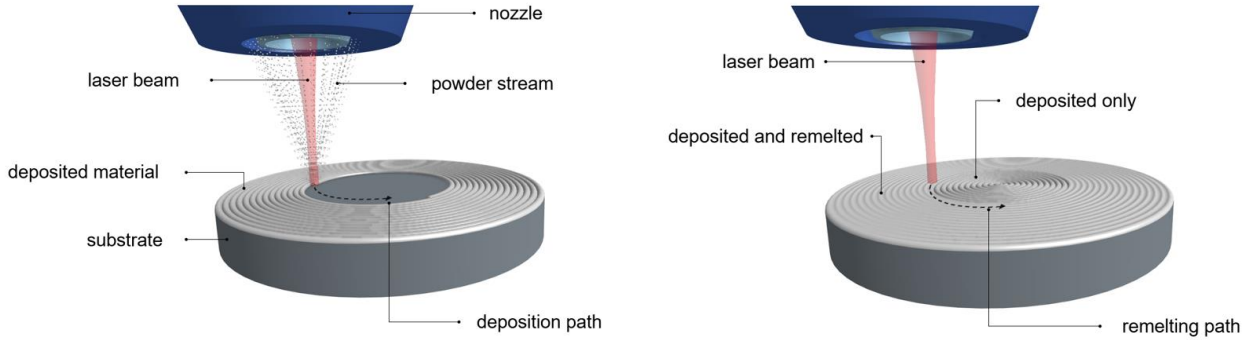

(a) (b)

Figure 2. Deposition and remelting of the coating. (a) Deposition process; (b) Remelting process.

In order to facilitate understanding, the coatings were divided into two categories: condition 1 - coating deposited only; condition 2 - coating deposited and treated by remelting. Figure 3 flowchart summarizes the steps carried out in the coatings manufacture.

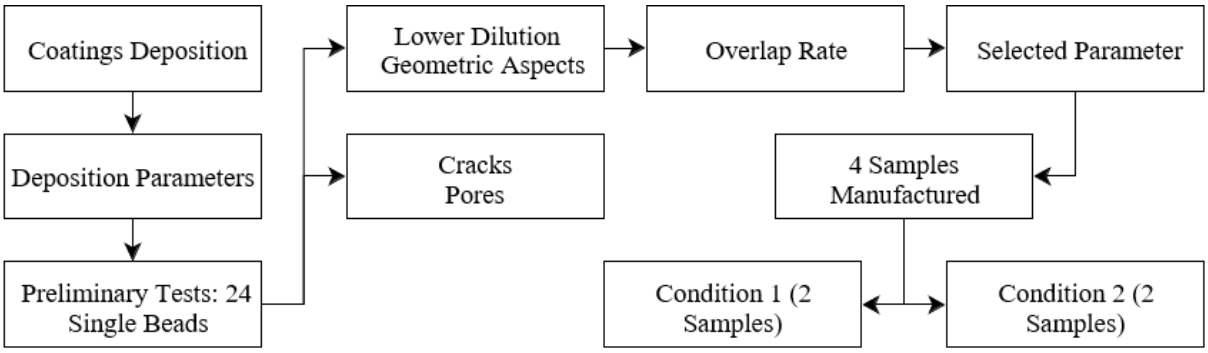

Figure 3. Flowchart of steps carried out in the coatings manufacture.

2.4 Microhardness test and dry pin-on-disk tribological test

Vickers microhardness test was performed in a sample, randomly chosen, from each condition using the SHIMADZU® HMV-2TADW equipment, according to the ASTM-E92 (2017) standard guidelines: HV_1 scale - 10 N load for 10 s. Indentations were applied in the coatings surface in corresponding regions to the later tribological test area (radial direction), as shown in Figure 4. Spacing between indentations was 5 and 7 mm for the radius 1 (15 mm) and radius 2 (18 mm), respectively.

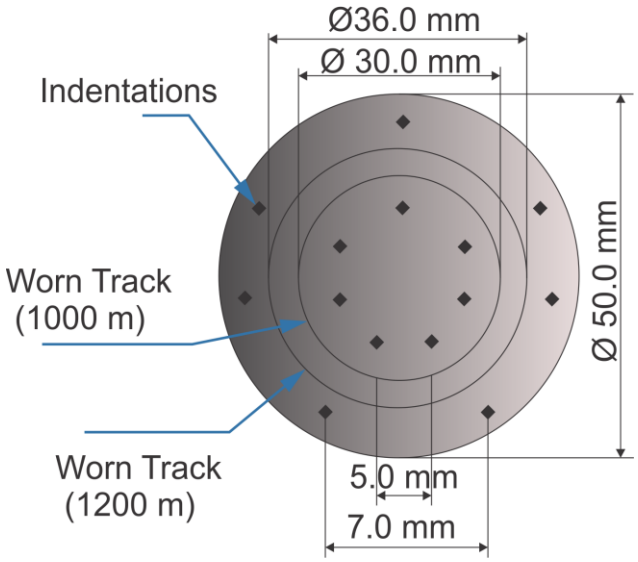

Figure 4. Sketch of performed Vickers microhardness indentations and worn tracks on the sample.

ASTM-G99 (2017) specifications related to size, dimensions and surface finish of the samples were met, as after coating, the samples were subjected to grinding, reaching the roughness value R_a = 0.8 µm. Before and after tribological test, samples were cleaned in ethyl alcohol, dried and weighed in a precision scale with ± 0.001 g resolution.

With the tribometer calibrated, the pin-on-disk test was carried out in dry medium, aiming to reproduce actual two bodies wear. The Ni-Cr-B-Si coated discs were used as body and the aluminum oxide ball (Al_2O_3 - Ø 6 mm) as counter body. The data generated in the tests was acquired through LABVIEW® software. Based in literature, the test parameters were chosen: normal load, 10 N; sliding speed, 0.5 m/s; as well as two sliding distance values: 1000 m and 1200 m. Relative humidity and ambient temperature were monitored during the tests (Houdková et al., 2014) and (Deschuyteneer et al., 2017).

From the experimentation performed, the following results were measured or calculated: Khruschov (1957) H_a/H ratio; volumetric loss (via optical interferometry); *k* coefficient through the Eq. (1) Archard (1953) model; friction coefficient (COF), measured by a load cell PW4MC3-30 N. The worn surfaces aspects and chemical composition were analyzed via scanning electron microscope (SEM) and energy dispersive spectroscopy (EDS) in a HITACHI® TMC 3030, respectively.

$$k = Q / (Ln*D) \quad (1)$$

where: Q = *volumetric loss* (mm^3); k = Archard's wear coefficient [$mm^3/(Nm)$]; Ln = normal load (N) and sliding distance (m).

3. RESULTS AND DISCUSSION

3.1 Surfaces aspects and coatings microhardness

The coatings presented good surface finish and resistant metallurgical adhesion between substrate and addition material. The final geometric aspects were consistent with the prediction made in MATLAB® software. In condition 1, some cracks were identified on the coating surface. Their disposition in parallel to the radius direction (deposition sense) indicates that they are resulting from high tensile stresses arising from cooling process. This problem was not identified in the samples that were submitted to laser remelting post-treatment.

In the literature, Houdková et al. (2014) highlighted that during remelting process, a remelted material portion is relocated by surface tension to the lower valleys in relation to the plane. Zhao et al. (2018) indicates that this phenomenon can be easily understood when it is thought that the material of the roughness peaks is driven into the valleys, filling them, leaving a smooth and more leveled surface. In this research case, the cooling cracks resultant from the deposition process have been filled by this phenomenon. Moreover, it can be concluded that as the remelting was applied immediately after deposition end, not enough time was allowed for significant temperature drop, thus such high thermal gradient was not present, which is the mainly responsible for cooling cracks nucleation and, therefore, no new cracks were developed.

Regarding microhardness values, the remelting treatment was also advantageous. Although the microhardness average (condition 1 - 582 HV_1 and condition 2 - 594 HV_1) difference between coatings conditions was small, punctual

microhardness values along the total indentations set performed were more pronounced in condition 2. The microhardness performance improvement is probably due to the internal void (like pores) reduction and to the increasing in internal coating cohesion. Houdková et al. (2014) and Sousa et al. (2018) observed similar behavior in their research, attributing it to these same justifications. Besides that, in the present research, this result may also be an indicative of the better reinforcement phases distribution (Cr carbides - CrC, identified via EDS) along the surface of condition 2 coating (subject best discussed in topic 3.3). Figure 5 graph describes the microhardness behavior.

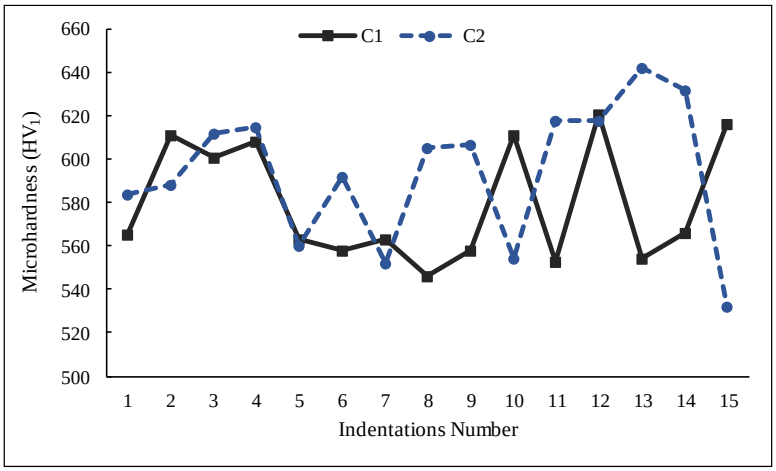

Figure 5. Coatings surface microhardness: C1 - condition 1 and C2 - condition 2.

3.2 COF, volumetric loss and *k* Archard's coefficient

From the Khruschov (1957) relationship, both conditions underwent a severe wear regime (condition 1 - H_a/H: 3.5 and condition 2 - H_a/H: 3.4). It is important to note that this relation considered the average overall hardness value of the coatings in their calculation. Thus, unlike the results obtained during the test (Figure 3), it is not possible to observe a significant difference. However, in real applications where a component is subjected to constant mechanical stresses, a better uniformity of the mechanical properties' distribution may be even more important than the overall H_a/H value. The graph of Figure 3 showed that the condition 2 was more efficient in this regard.

The COF average over the test time for both conditions and sliding distances analyzed (1000 and 1200 m) was very similar (approximately 0.5). However, remelting treatment application contributed to the COF variation reduction along the test. Standard deviation analysis indicated, at both sliding distances evaluated, approximately 20% lower variation in the condition 2 in relation to condition 1. Similar results are reported by García et al. (2016) and Zhao et al. (2018).

Although condition 1 samples showed an inversely proportional behavior between microhardness and wear rate, this behavior was more pronounced in the condition 2. Thus, it is believed that the higher internal coating cohesion improved by remelting treatment also had a direct impact on this result. In the literature, Yin et al. (2011) and Zhao et al. (2018) report similar results. Figure 6 shows the volumetric loss for the different test sliding distances.

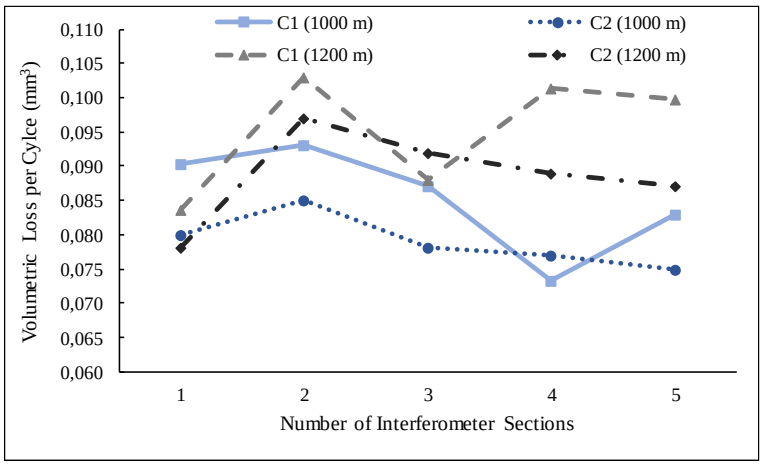

Figure 6. Resultant volumetric loss for both conditions and sliding distances: C1 - condition 1 and C2 - condition 2.

The graph of Figure 7 shows the cumulative average volumetric loss over the total test time, where it is possible to perceive the difference in a more quantitative way. In both sliding distances analyzed, condition 1 presented a performance clearly inferior to condition 2. Besides that, condition 2 standard deviation was smaller than that of condition 1, which indicates its better uniformity of mechanical and tribological properties distribution along the coating thickness, corroborating also its lower volumetric loss evaluated punctually in the graph of Figure 4.

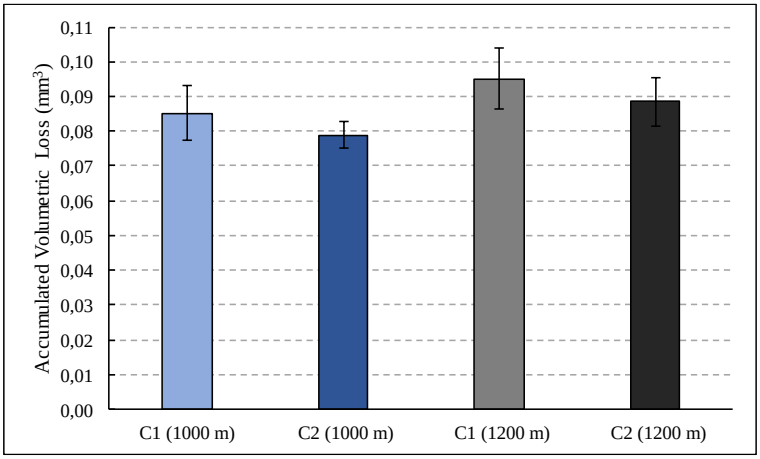

Figure 7. Accumulated volumetric loss over the total test time: C1 - condition 1 and C2 - condition 2.

As the load and sliding distance were kept constant, the *k* Archard coefficient presented correlation with the volumetric loss results bellow at Figure 7. However, some particularities can be observed in relation to the volumetric loss (Figure 6). First, condition 2 coating presented lower *k* values at most of the measurement points, whereas in Figure 6, this behavior was only identified for 1000 m sliding distance. Besides that, in Figure 6, volumetric loss was higher in the condition 1 at 1200 m sliding distance and lowest for the condition 2 at 1000 m sliding distance. In Figure 8, on the other hand, the highest *k* coefficient was for condition 1 at 1200 m sliding distance and the lowest was for the condition 2 at 1200 sliding distance.

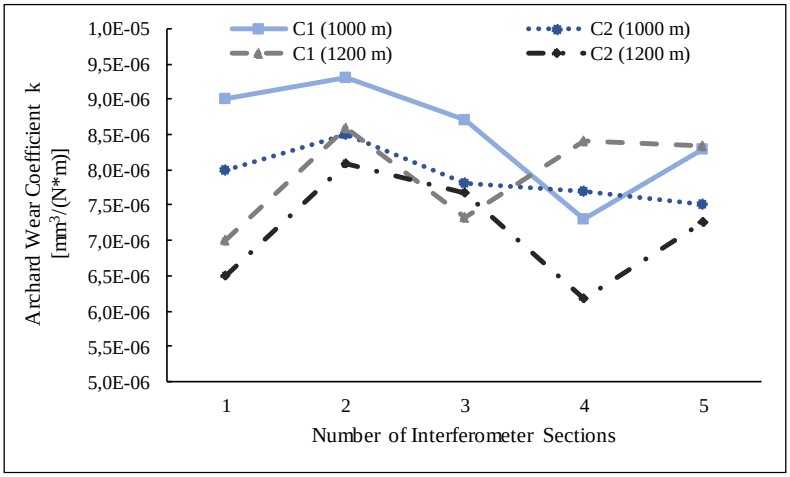

Figure 8. Archard wear coefficient for both conditions and sliding distances: C1 - condition 1 and C2 - condition 2.

In general, the remelting treatment application reduced volumetric loss and *k* coefficient by approximately 12%. This result was observed at both sliding distances analyzed. This behavior proved to be compatible with surface characteristics, hardness and defects absence. The punctual variations found, especially in Figure 8, are probably related to the wear micromechanisms behavior that acted on the tribological pair. This and the other interactions identified will be further discussed throughout topic 3.3.

3.3 Worn surfaces analysis

Figure 9 shows worn surfaces of the coatings with and without remelting treatment, highlighting the wear micromechanisms types identified: (a) condition 1 coating worn surface shows adhesive wear, microploughings, chromium carbides (CrC), tribolayers and coating detachment; (b) condition 2 coating worn surface, on the other hand, presents only CrC and a few adhesion and oxidation points.

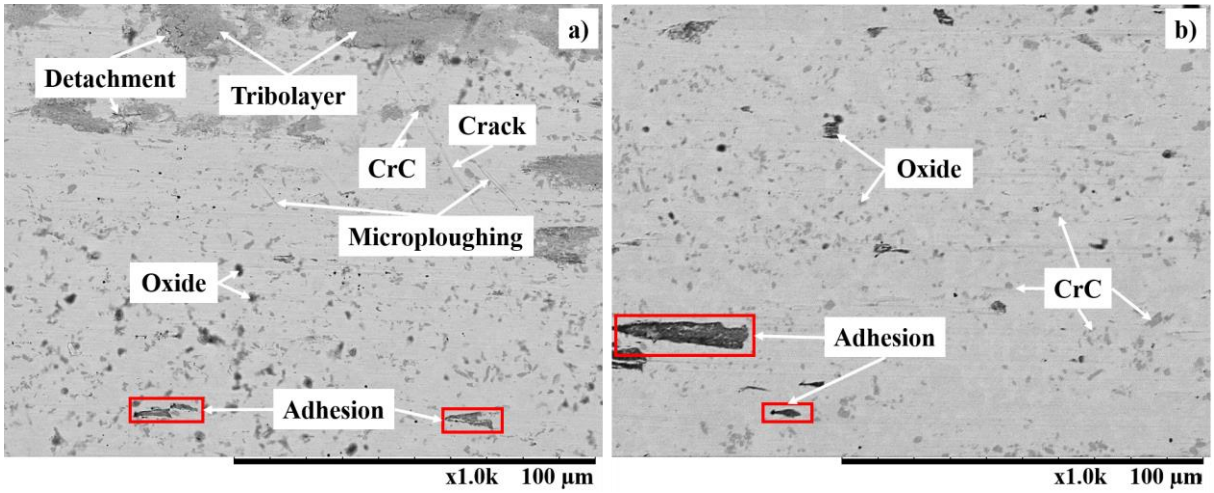

Figure 9. Worn surfaces images (1000 m sliding distance) obtained via MEV: a) condition 1 and b) condition 2.

Analyzing Figure 9, characteristic two bodies wear micromechanisms, adhesion and oxides are noticed in both the analyzed conditions. However, the action of these was more pronounced in condition 1 that, besides to these, presented other mechanisms including characteristics of three bodies wear, like microploughing. In Figure 9a, although there are fractured CrC phases, there is no clear microcuttings evidence. As these phases have a much higher hardness than the matrix, loose particles acting as interfacial element could have increased the wear severity.

As for CrC precipitates, in both conditions, no significant difference was identified regarding the concentration and size of these. However, in condition 2 (Figure 9b), CrC phases were better distributed along the surface in relation to condition 1 (Figure 9a). This factor, added higher microstructure refinement provided by remelting, were essential to increase the coating surface hardness, making it difficult for the sphere to penetrate in these surfaces. Besides that, CrC adhesion to the matrix was more efficient, avoiding phases detachments and increasing the restraint effect, which interrupts and/or hampers microploughings advancement; a phenomenon that goes back to Zum Gahr (1987) model. In the literature, similar results regarding the reinforcement phases behavior are indicated in several works, Houdková et al. (2014), (Férnandez et al., 2015), (García et al., 2016), (Deschuyteneer et al., 2017) and (Sousa et al., 2018).

Figure 9 also made it clear that the active wear micromechanisms action was relatively contained from condition to the other. However, two factors identified only in condition 1 indicated the main causes of the higher wear rate presented then: tribolayers detachment and coating material detachment close to the cooling cracks.

In the literature, it is found that the tribolayers presence is advantageous due to its lubricating effect, where they act as interfacial element, reducing the direct contact between body and counter body (Hutchings; Shipway, 2017). There are experimental studies that indicate the observation of this behavior (Da Silva; D'Oliveira, 2016). In this research, these elements presence, identified only in condition 1 for 1000 m sliding distance, contributed to the COF stabilization. However, tribolayers detachment was identified as a significant detrimental influence on their wear rate. Although no tribolayers was detected for 1200 m sliding distance, as the wear rate of both sliding distance was similar, it is believed that these tribolayers were removed along test time through the tribological pair interaction, and not by removal of more coating material. Similar result was found by Sousa et al. (2018). Figure 10a shows an approximate image of condition 1's worn surface, where it is possible to perceive: 1 - tribolayer Detachment, 2 - cooling cracks and 3 - coating material detachment close to the latter. Figure 10b shows an EDS spectrum, indicating the oxidation generated in this region.

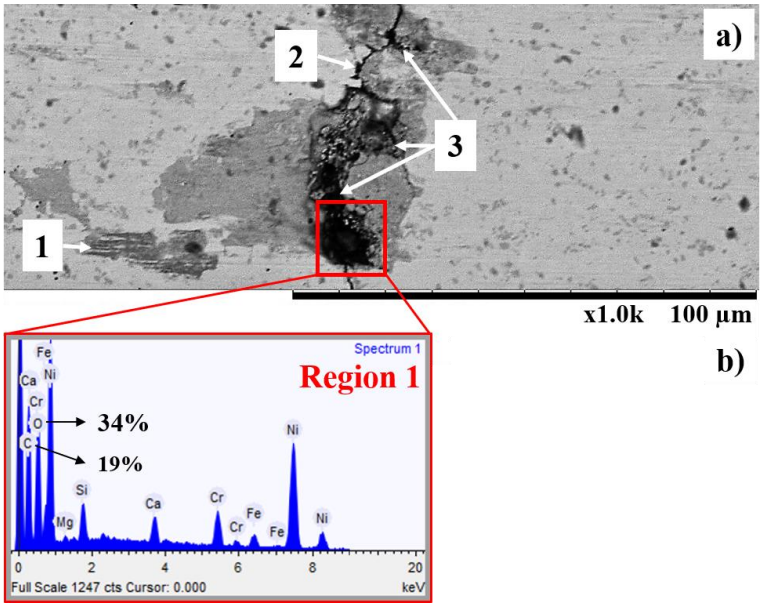

Figure 10. Worn surface: a) 1 - tribolayer detachment, 2 - cooling cracks and 3 - coating material detachment close to the cooling cracks; b) EDS spectrum.

Figure 10 made it clear that the cooling cracks impaired the coating performance of condition 1 in relation to condition 2. The presence of this defect caused detachment of coating and counter body material through the collision between the tribological pair at the time the sphere goes through a cracked region, generating vibration, which increased COF variation. As the test proceeds, debris accumulation within the cooling cracks has generated fatigue collapses at these interfaces, removing coating fragments. The deteriorated ball surface wore out the coating surface more severely, increasing volumetric loss and *k* coefficient. Besides that, part of the generated debris ended up being loose between tribological pair, establishing a three bodies wear interface, that may have generated a considerable part of the microploughings observed in Figure 9a.

Cooling cracks absence in condition 2 is due to the lower thermal gradient provided by remelting, which reduced tensile stresses of the cooling process, which is the nucleation source of these cracks. In this way, remelting treatment eliminated all the damage defects originating from these defects, the most severe of which is the material removal and embrittlement of the coating. In the literature, several researches report obtaining similar problems arising from the cooling cracks presence in the coatings of this alloy class. A technique widely used to avoid nucleation of these cracks is the application of substrate preheating at different temperatures, (Houdková et al., 2014), (Férnandez et al., 2015) and (García et al., 2016). Remelting application is also evaluated in this sense, (Lim, 2011) and (Yin et al., 2011). There are also studies that analyze coatings without treatments, investigating the cooling cracks effects on tribological behavior in a more extensive way, (Sousa et al., 2018).

In the optical interferometry analysis, used in the worn tracks volume loss evaluation, it is possible to notice that the worn tracks characteristics corroborate the values of volumetric loss and *k* coefficient. The area removed from condition 2 was lower than condition 1. Maximum average worn track depth of condition 2 (10 µm) was also lower than that of condition 1 (13 µm). Besides that, worn track irregularity of condition 1 was also higher in relation to condition 2, a result that may be related to the cooling cracks and the removal of some CrC phases present on its surface, which generated abrasion. This factor also reveals higher uniformity on the surface treated by remelting. Higher penetration depth and higher worn track irregularity of condition 1 corroborate the values of volumetric loss and *k* coefficient, presented previously in the graphs of Figure 5, 6 and 7, respectively. Figure 11 shows worn tracks characteristic sections, both for 1000 m sliding distance: a) condition 1 and b) condition 2.

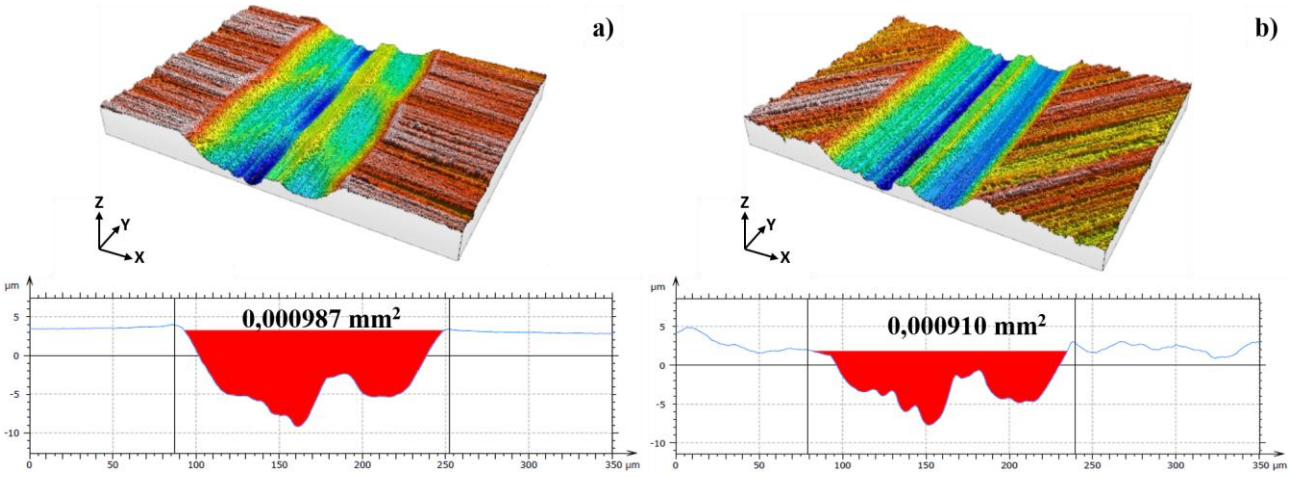

Figure 11. Track sections worn for 1000 m sliding distance: a) condition 1 and b) condition 2.

In both conditions of coating and sliding distances evaluated, there was no significant difference in wear of the spheres used as counter body. Thus, it is possible to infer that only material removed from the coating contributed to the tribolayers formation, the effects of which were previously described. As shown in Figure 12, in the spheres body, three phenomena were identified: coating adhesion (more and less severe); detachment and re-adhesion of the sphere material itself (Al_2O_3); and less severe adhesion regions (Figure 12a), probably due to direct contact between CrC phases or cooling cracks during the test. In literature, Férnandez et al., (2015) highlights the achievement of similar results. Diameter of the worn shell was practically equal in both conditions evaluated.

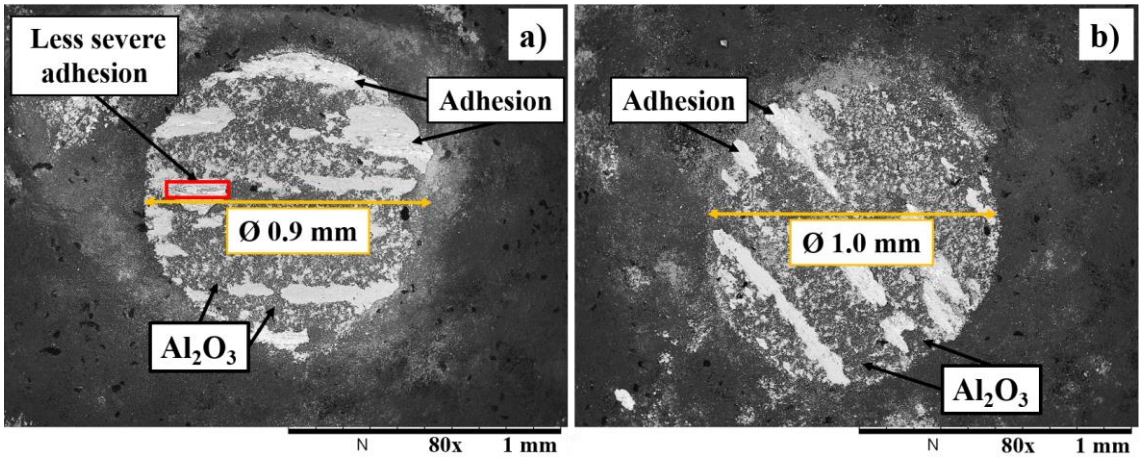

Figure 12. Worn surface of balls used as counter body: a) condition 1 and b) condition 2.

In evaluation of the debris generated along the tribological tests (Figure 13a), a great dispersion of morphology and size was observed, where no characteristic patterns were identified. By the Khruschov (1957) ratio, both coatings conditions evaluated presented severe wear regime, a factor that might have contributed to this result. EDS spectrum of these (Figure 13b) revealed metallic oxides aspects, category to which they are attributed in the literature, (Da Silva; D'Oliveira, 2016) and (Sousa et al. 2018).

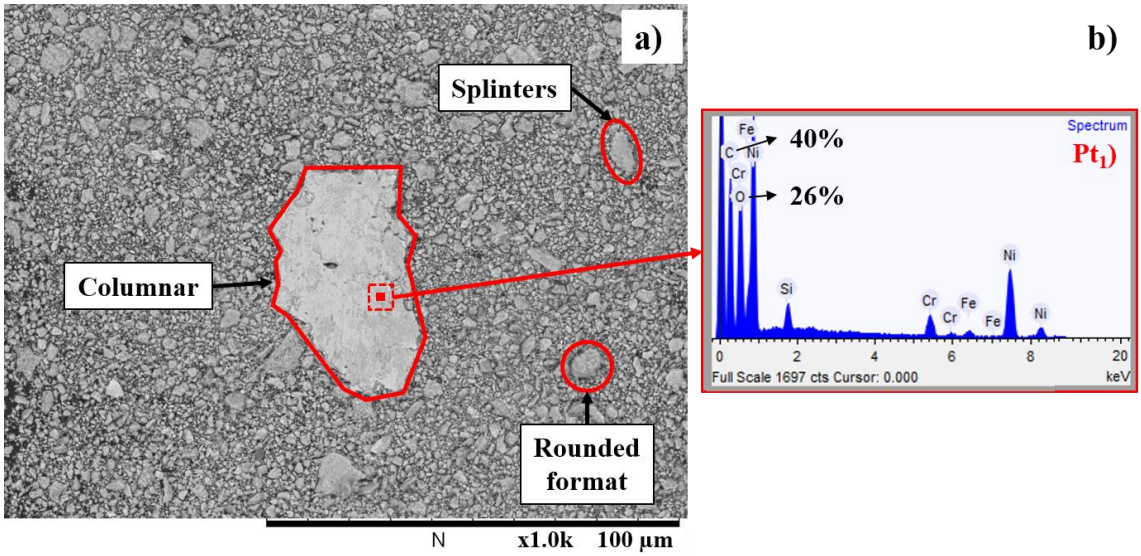

Figure 13. Debris generated during the tribological test: a) general characteristics and b) EDS spectrum.

In general, the various aspects evaluated of worn surfaces are consistent with results of surface characteristics, hardness and tribological behavior.

4. CONCLUSIONS

From the results obtained in the coatings' analysis in relation to their general aspects, microhardness, tribological behavior and worn surfaces, it was concluded that:

- The laser remelting post surface treatment exerted a beneficial effect in coating internal cohesion enhancement, microstructure refinement, distribution of Cr carbides, microhardness increases and cooling cracks reduction.
- Friction coefficient average did not present significant changes. However, its variation was reduced by remelting.
- The sum of the variables improved by remelting culminated in the reduction of volumetric loss and *k* coefficient.
- Worn surfaces analysis corroborated results above, presenting a significantly less severe appearance in the remelted coating.
- Tribolayers presence tends to decrease with sliding distance increase. Besides this exception, difference in sliding distance did not present significant influence on any of the other evaluated characteristics.
- Worn tracks analyzed via optic interferometry presented characteristics compatible with the other wear analysis, where the average depth and irregularities of the worn tracks was less pronounced in the remelted coating.
- Counter body wear was similar in both coatings' conditions. Debris did not present a defined pattern of morphology and size.
- The sum of the detachment of tribolayers and coating material close to the cooling cracks was identified as the main influence on the differences between the tribological performances.

5. AKNOWLEDGEMENTS

The Universidade Federal de Santa Catarina (UFSC) and SATC College by scientific technical support. The Coordination for the Improvement of Higher Education Personnel (CAPES) and National Council for Scientific and Technological Development - CNPq for financial support.

6. REFERENCES

Archard, J. 1953. "Contact and rubbing of flat surfaces". *Journal of applied physics***,** Vol. 24, pp. 981-988.

ASTM-E92. 2017. *American Society for Testing and Materials: Standard Test Methods for Vickers Hardness and Knoop Hardness of Metallic Materials.* ASTM, Pensilvânia. Pensilvânia, 27 p. 2017.

ASTM-G99. 2017. *American Society for Testing and Materials: Standard Test Method for Wear Testing with a Pin-on-Disk Apparatus.* ASTM, Pensilvânia.

Da Silva, L.J. and D'Oliveira, A.S.C.M., 2016. "NiCrSiBC coatings: Effect of dilution on microstructure and high temperature tribological behavior". *Wear***,** Vol. 350, pp. 130-140.

Davim, J.P., 2013. *Laser in manufacturing*. John Wiley & Sons, New Jersey, 1nd edition.

Deschuyteneer, D., Petit, D., Gonon, M. and Cambier, F. "Influence of large particle size – up to 1.2mm – and morphology on wear resistance in NiCrBSi/WC laser cladded composite coatings". *Surface & Coatings Technology*, Vol. 311, pp. 365-373.

Férnandez, M.R., García, A., Cuetos, J.M., González, R., Noriega, A. and Cadenas, M. "Effect of actual WC content on the reciprocating wear of a laser cladding NiCrBSi alloy reinforced with WC". *Wear*, Vol. 324-325, pp. 80-89.

García, A., Férnandez, M.R., Cuetos, J.M., González, R., Ortiz, A. and Cadenas, M. "Study of the Sliding Wear and Friction Behavior of WC + NiCrBSi Laser Cladding Coatings as a Function of Actual Concentration of WC Reinforcement Particles in Ball-on-Disk Test". *Triboll Lett*, Vol. 41.

Gusarov, A.V., Pavlov, M. and Smurov, I. "Residual Stresses at Laser Surface Remelting and Additive Manufacturing". *Physics Procedia*, Vol. 12, pp. 248-254.

Houdková, Š., Smazalová, E., Vostřák, M. and Schubert, J., 2014. "Properties of NiCrBSi coating, as sprayed and remelted by different technologies". *Surface and Coatings Technology***,** Vol. 253, pp. 14-26.

Hutchings, I.; Shipway, P., 2017. *Tribology: friction and wear of engineering materials*. Butterworth-Heinemann, Cambridge, 1nd edition.

Khruschov, M.M. 1957. "Resistance of Metals to Wear by Abrasion, as Related to Hardness". *Lubrication and Wear*, Vol. 655.

Marimuthu, S., Triantaphyllou, A., Antar, M., Wimpenny, D., Morton, H. and Beard, M., 2015. "Laser polishing of selective laser melted components". *International Journal of Machine Tools & Manufacture*, Vol. 95, pp. 97-104.

Ocelík, V., Nenadl, O., Palavra, A. and De Hosson, J.Th.M., 2014. "On the Geometry of Coatings Layers Formed by Overlap". *Surface & Coatings Technology*, Vol. 242, pp. 54-61.

Sousa, J.M.S., Ratusznei, F., Pereira, M., Castro, R.M. and Curi, E.I.M., 2018. "Abrasion Resistance of Ni-Cr-B-Si Deposited by Laser Cladding Process". *In Proceedings of the 3nd International Brazilian Conference on Tribology - TRIBOBR 2018.* Florianópolis, Brazil.

Temmler, A., Willenborg, E. and Wissenbach, K., 2015. "Design surfaces by laser remelting". *Materialwissenschaft und Werkstofftechnik*, Vol. 46, pp. 692-703.

Toyserkani, E., Corbin, S., Khajepour, A. 2005. *Laser Cladding*. CRC Press LLC, Florida, 1nd edition.

Yin, B., Zhou, H.D, Chen, J.M. and Yan, F.Y., 2011. "Microstructure and high temperature sliding wear behaviour of laser remelted NiCrBSi/35(WC-12Ni) composite coating". *Surface Engineering***,** Vol. 27, pp. 458-463.

Zhao, Y., Sun, J., Guo, K. and Li, J., 2018. "Investigation on the effect of laser remelting for laser cladding nickel based alloy". *In Proceedings of the 37nd International Congress on Applications of Lasers & Electro-Optics – ICALEO 2018.* Orlando, United States of America.

Zhong, M. and Liu, W., 2010. "Laser surface cladding: the state of the art and challenges". *Journal of Mechanical Engineering Science***,** Vol. 224, pp. 1041-1060.

Zum Gahr, K.-H. *Microstructure and ear of materials*. Elsevier Science, New York, 1nd edition.

7. RESPONSIBILITY NOTICE

The authors are the only responsible for the printed material included in this paper.